

**ICSO 2016**

**International Conference on Space Optics**

Biarritz, France

18–21 October 2016

*Edited by Bruno Cugny, Nikos Karafolas and Zoran Sodnik*



***Radiometric characterization of type-II InAs/GaSb superlattice (t2sl) midwave infrared photodetectors and focal plane arrays***

*Jean Nghiem*

*E. Giard*

*M. Delmas*

*J. B. Rodriguez*

*et al.*



International Conference on Space Optics — ICSO 2016, edited by Bruno Cugny, Nikos Karafolas, Zoran Sodnik, Proc. of SPIE Vol. 10562, 105623Y · © 2016 ESA and CNES  
CCC code: 0277-786X/17/\$18 · doi: 10.1117/12.2296053

## RADIOMETRIC CHARACTERIZATION OF TYPE-II INAS/GASB SUPERLATTICE (T2SL) MIDWAVE INFRARED PHOTODETECTORS AND FOCAL PLANE ARRAYS

J.Nghiem<sup>1</sup>, E.Giard<sup>1</sup>, M. Delmas<sup>2,3</sup>, J.B.Rodriguez<sup>2,3</sup>, P.Christol<sup>2,3</sup>, M.Caes<sup>1</sup>, H.Martijn<sup>4</sup>, E.Costard<sup>4</sup>, I.Ribet-Mohamed<sup>1</sup>

<sup>1</sup>ONERA/DOA, F-91761, Palaiseau, France

<sup>2</sup>Univ. Montpellier, IES, UMR 5214, F- 34000, Montpellier, France

<sup>3</sup>CNRS, IES, UMR 5214, F- 34000, Montpellier, France

<sup>4</sup>IRnova AB, Electrum 236, SE-164 40 KISTA, Sweden

### I. INTRODUCTION

In recent years, Type-II InAs/GaSb superlattice (T2SL) has emerged as a new material technology suitable for high performance infrared (IR) detectors operating from Near InfraRed (NIR, 2-3 $\mu$ m) to Very Long Wavelength InfraRed (LWIR,  $\lambda > 15\mu$ m) wavelength domains.

To compare their performances with well-established IR technologies such as MCT, InSb or QWIP cooled detectors, specific electrical and radiometric characterizations are needed: dark current, spectral response, quantum efficiency, temporal and spatial noises, stability...

In this paper, we first present quantum efficiency measurements performed on T2SL MWIR (3-5 $\mu$ m) photodiodes and on one focal plane array (320x256 pixels with 30 $\mu$ m pitch, realized in the scope of a french collaboration). Different T2SL structures (InAs-rich versus GaSb-rich) with the same cutoff wavelength ( $\lambda_c = 5\mu$ m at 80K) were studied. Results are analysed in term of carrier diffusion length in order to define the optimum thickness and type of doping of the absorbing zone.

We then focus on the stability over time of a commercial T2SL FPA (320x256 pixels with 30 $\mu$ m pitch), measuring the commonly used residual fixed pattern noise (RFPN) figure of merit. Results are excellent, with a very stable behaviour over more than 3 weeks, and less than 10 flickering pixels, possibly giving access to long-term stability of IR absolute calibration.

### II. InAs/GaSb T2SL QUANTUM STRUCTURE

A superlattice (SL) is a periodic stack of thin heterostructures, ie interfaces between two layers of different semiconductors. The InAs/GaSb heterointerface features a specific type-III band alignment, where the valence band of the GaSb layer is higher than the conduction band of the InAs layer, as shown in Fig 1a. Each GaSb/InAs/GaSb block acts as a quantum well, thus this structure can be viewed as a system of coupled multi quantum wells. Electrons are then confined in minibands of energy instead of discrete levels.

The bandgap of this periodic structure is defined by the energy difference between the first electron miniband C1 and the first heavy hole miniband V1 as illustrated in Fig 1, and depends on the thicknesses of the InAs and GaSb layers.

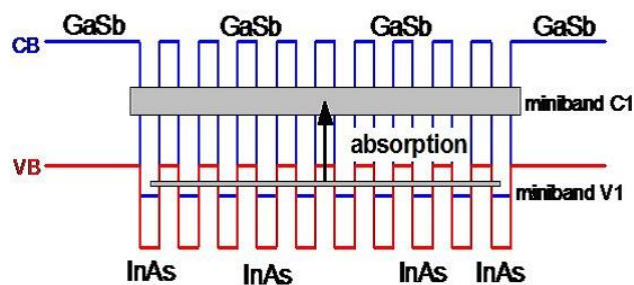


Fig 1 Schematic InAs/GaSb SL structure displaying the fundamental electron C1 and heavy hole V1 minibands. The absorption of infrared photons occurs between these two minibands.

The SL can absorb a wide range of IR wavelengths by engineering the bandgap (3 $\mu$ m to 30  $\mu$ m wavelengths) without changing the fabrication process. Fig 2 shows the photoresponse spectra of symmetric

InAs/GaSb T2SL, ie with the same number of InAs and GaSb monolayers (ML) in a period. It proves that T2SL can properly address the MWIR domain.

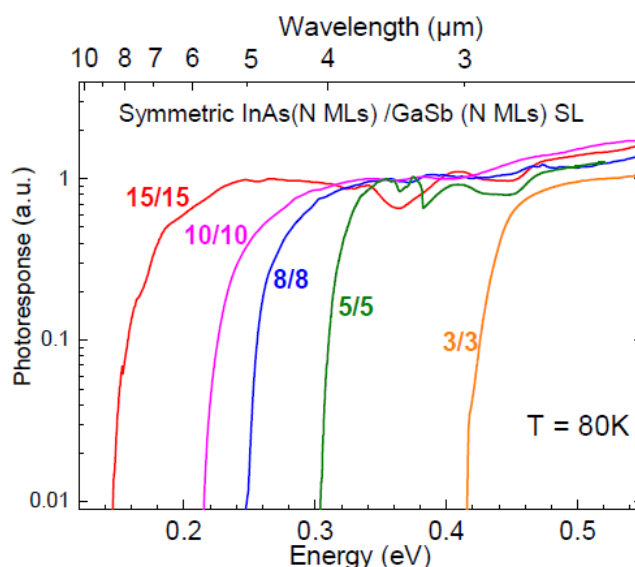


Fig 2 Normalized photoresponse spectra of InAs (N) /GaSb (N) symmetrical SL MWIR detector structures with N = 3, 5, 8, 10 and 15 MLs (1ML is 3Å thick). The spectra are recorded at 80 K.

### III. QUANTUM EFFICIENCY MEASUREMENTS

#### A. Comparisons of several T2SL structure designs

Comparisons are first made with 3 monoelement structures that have the same active zone thickness of 1μm, as seen in Fig. 3. They were made by Molecular Beam Epitaxy (MBE) using GaSb as substrate and were designed in order to have the same wavelength cutoff ( $\lambda_c=5\mu\text{m}$ ). Sample A is GaSb-rich, with a period made of 10ML of InAs and 19 ML of GaSb (10/19). Sample B is symmetric (10/10). Sample C is InAs-rich (7/4). Quantum Efficiency (QE) measurements have been performed at 0V bias voltage on these 3 structures. First the relative photoresponse was measured using a FTIR spectrometer and then the absolute QE was calibrated using a SR200 blackbody [1].

The QE results were compared in Fig. 3. At  $\lambda=4.5\mu\text{m}$ , better QE values were obtained by the symmetric and GaSb-rich SL structures while the absorption is higher in the InAs-rich design because of its large electron–holes wave-function overlap.

To explain why the QE of the InAs-rich structure is unexpectedly much lower than the other two, measurements at  $\lambda=4.5\mu\text{m}$  were analysed as a function of the bias voltage. Results are also shown in Fig 3. Increasing the bias voltage improves QE for the InAs-rich structure. It increases linearly from 6% to 17% by changing the bias voltage from 0V to -1V and then saturates. On the contrary, the QE of the GaSb-rich structures is independent of the bias voltage

The photocurrent is created in two steps: photon absorption (which creates the electron/hole pair) and collection of those carriers. The fact that increasing the bias voltage also improves the QE means that there is a problem of transport in the InAs-rich structure.

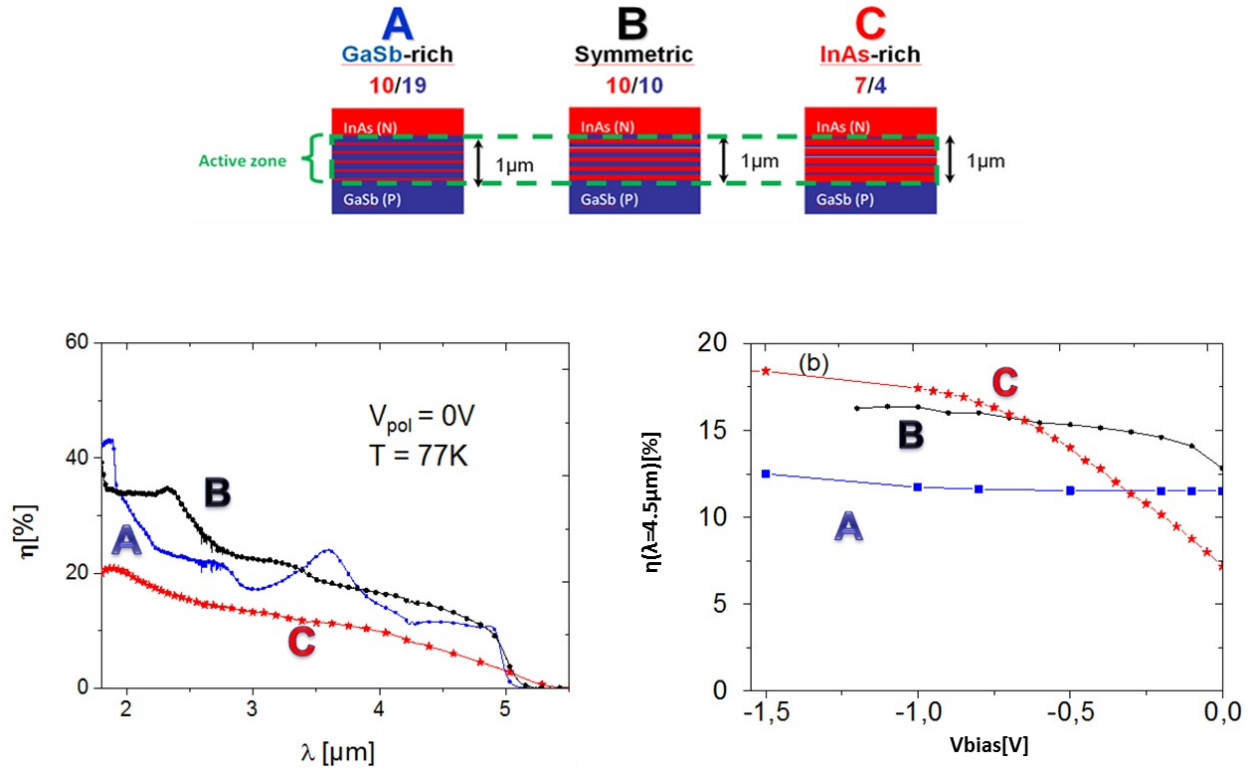


Fig 3 Right : Comparison of quantum efficiency of 3 different T2SL photodiodes at 77K. Left : QE as a function of the wavelength, for  $V_{bias}=0V$  ; right : QE as a function of the bias, for  $\lambda=4.5\mu m$ .

Simulations using Hovel equations [2][3] have been performed in order to determine the minority carrier diffusion length. QE is the sum of the contributions of three zones: the quasi neutral zone N (QEn), the depletion zone (QEzce) and the quasi neutral zone P (QEp).

$$QE = QE_n + QE_{zce} + QE_p \quad (1)$$

With:

$$QE_{zce} = (1 - R) * (e^{-\alpha x_1} - e^{-\alpha x_2}) \quad (2)$$

$$QE_p = \frac{(1 - R)\alpha L_e}{\alpha^2 L_e^2 - 1} e^{-\alpha x_2} * \left( \frac{\alpha L_h - \sinh\left(\frac{x_{max} - x_2}{L_h}\right) e^{-\alpha x_1}}{\cosh\left(\frac{x_{max} - x_2}{L_h}\right)} + \alpha L_e \right) \quad (3)$$

$$QE_n = \frac{(1 - R)\alpha L_h}{\alpha^2 L_h^2 - 1} * \left( \frac{\alpha L_h - \sinh\left(\frac{x_1}{L_h}\right) e^{-\alpha x_1}}{\cosh\left(\frac{x_1}{L_h}\right)} - \alpha L_h e^{-\alpha x_1} \right)_p \quad (4)$$

Where  $\alpha$  is the absorption coefficient, set equal to  $2200 \text{ cm}^{-1}$  [4];  $L_e$  and  $L_h$  are the electron and hole diffusion lengths respectively, with  $L_e$  set equal to  $6\mu m$  [5].  $R$  is the reflectance at the air/T2SL interface and set equal to 0.3.  $x_1$  and  $x_{max}-x_2$  the thickness of the quasi neutral zone N and the quasi neutral zone P and depend on the bias voltage.

The InAs-rich SL structure is n-type residual with hole minority carriers [6]. We determined the hole diffusion length  $L_h$  by fitting the equation with the measured QE, using  $L_h$  as the only adjustable parameter. Fig 4 shows the QE simulation at  $V_{bias}=0$  and  $T=77K$  for three InAs-rich samples with three different active zone thicknesses equal to 500nm,  $1\mu m$  and  $4\mu m$ . The best agreement of the measured QE curves with Hovel equations was obtained with  $L_h=80nm$ . This poor value in diffusion length does not allow the hole minority carriers to reach the collection zone and then penalizes the QE.

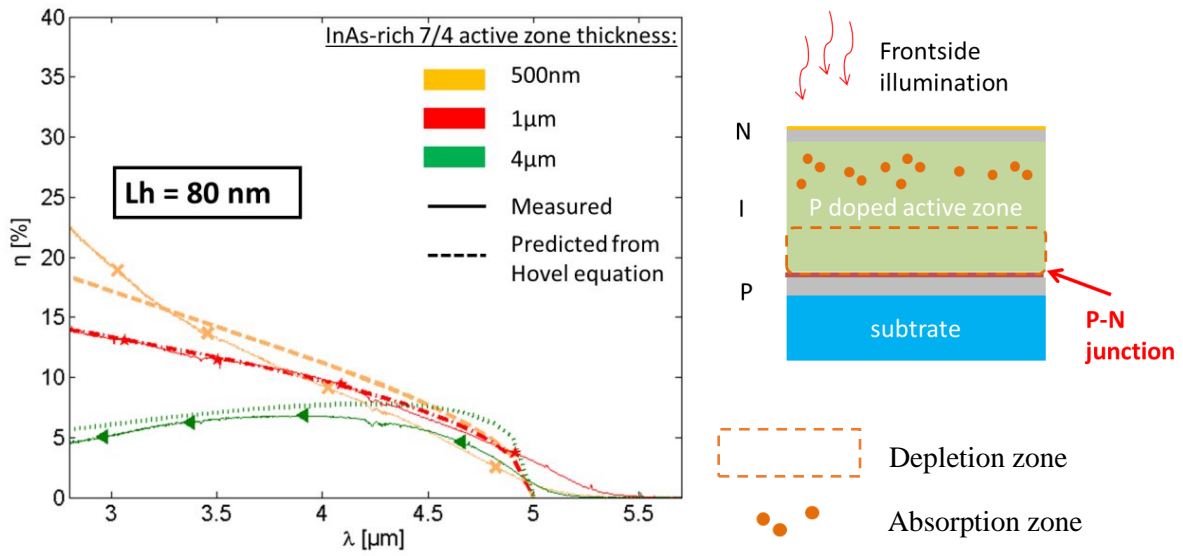


Fig 4 Left : comparison between QE measurements and predictions from Hovel equations for three InAs-rich photodiodes with different active zone thicknesses (500  $\mu\text{m}$ , 1  $\mu\text{m}$  and 4  $\mu\text{m}$ ), at 77K and 0V bias voltage; Right : schematic view of the front-side illuminated InAs-rich photodiode.

B. Conclusions

In the InAs-rich structure, the active zone features a residual N-type doping, meaning that the minority carriers are holes. As holes have a short diffusion length, the collection process is not optimal. One solution would be to change the minority carriers into electrons, which have a better diffusion length [6]. This can be done by slightly P-doping the active zone, leading to a P<sup>+</sup>PN junction as used in [7] to optimize LWIR structures. Fig 5 displays the QE comparison between intentionally P doped and non intentionally doped (nid) N-type residual InAs-rich photodiodes (7/4, 4 $\mu\text{m}$  active zone thickness, front side illuminated). We note that the measured QE is enhanced by up to 10 times by P-doping the InAs-rich T2SL (40% QE efficiency at  $\lambda=4.5\mu\text{m}$  for the P doped structure). To complete the comparison, QE measurements as a function of bias voltage are also plotted. In the P doped structure, we can see that the QE does not vary with the bias voltage, staying at 40% for  $\lambda=4.5\mu\text{m}$ , highlighting an optimised collection of electron minority carriers in p-doped InAs-rich T2SL structure.

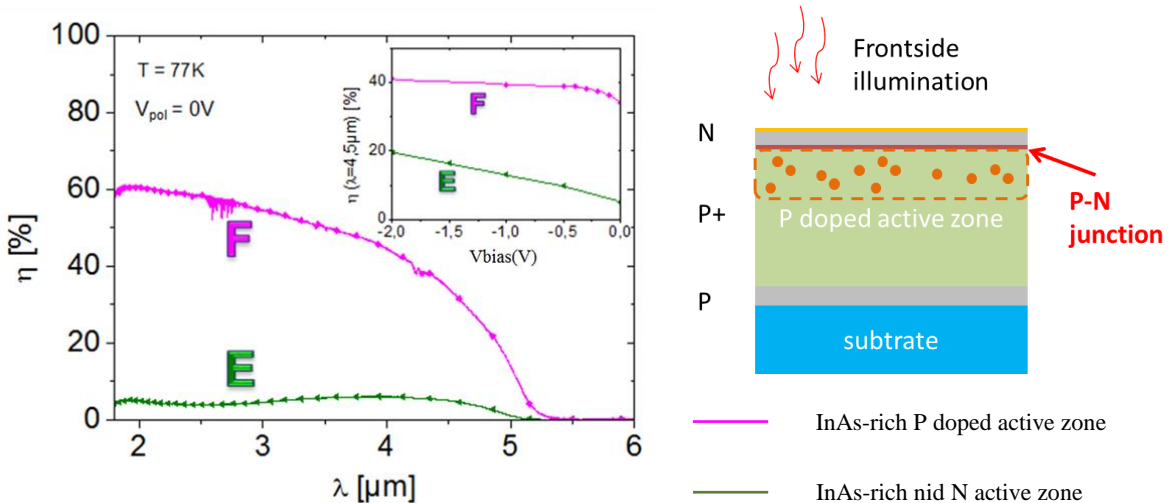


Fig 5 Left : QE measurements on InAs-rich T2SL photodiodes with non intentionally doped or P doped active zone at 77K and  $V_{bias}=0\text{V}$  ; Right : schematic view of the front-side illuminated InAs-rich photodiode (the p-n junction is now at the i/n interface, allowing a good overlap between the absorption and the collection zones).

Another solution to improve the QE is to ensure that the holes are created closer to the P/N junction, by backside illuminating the T2SL just like the FPA configuration. Fig 6 represents the QE measurement of an InAs-rich nid MWIR FPA (320x256) made in France [2]. The 42% average QE is due to the fact that this structure is double-pass and that the depletion zone is now better overlapping with the absorption zone, which allows more hole minority carriers to be collected.

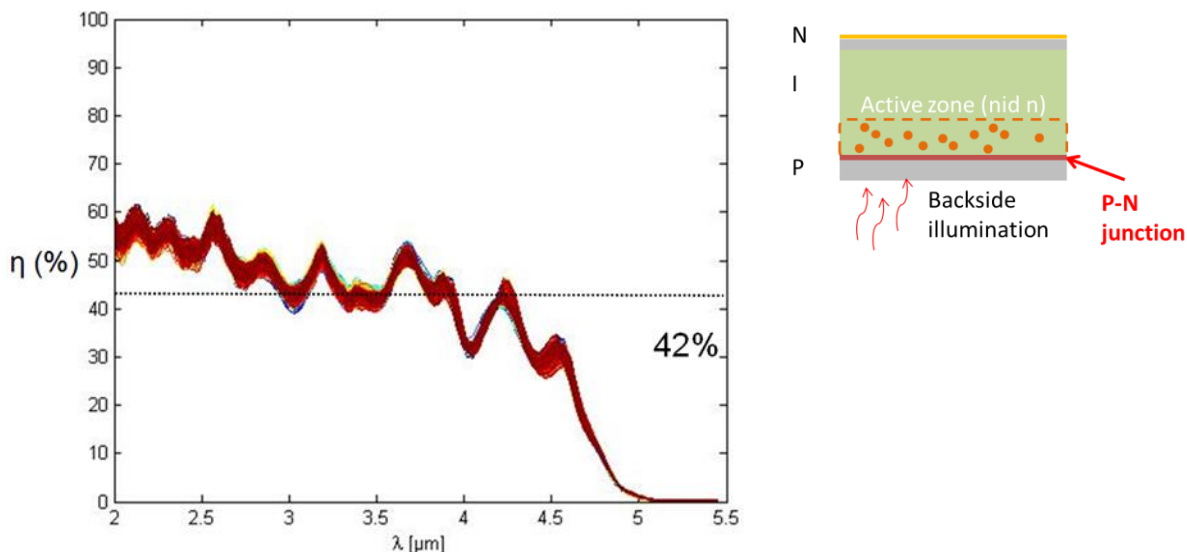


Fig 6 Left : QE measurements on InAs-rich MWIR FPA (320x256) at 77K on 600 pixels at the center; right : schematic view of the back-side illuminated InAs-rich photodiode (the p-n junction is now at the p/i interface, allowing a good overlap between the absorption and the collection zones).

#### IV. STABILITY OVER TIME AND CORRECTABILITY

Regardless of the applications, uniformity and stability over time of FPAs have been key priorities and recent works on flickering pixels [8] prove that they are still relevant. The usual approach to evaluate them is through estimating the Residual Fixed Pattern Noise (RFPN) and the number of flickering pixels.

##### A. Residual Fixed Pattern Noise

Spatial noise is due to various physical effects that can appear in the photodiode itself, in the readout circuit or during the technological steps of hybridization. It results in the fact that pixels' response is not absolutely identical in an FPA. By using a gain/offset correction table, it is possible to damp the impact of those non-uniformities.

In order to obtain the gain/offset table, we used a Two Point Correction (TPC). It consists in the use of a blackbody at two fixed fluxes, or rather at two temperatures  $T_{bb}$  with radiances  $L_{bb}$  given by Planck's law for a blackbodies:

$$L_{T_{bb}}(T_{bb}) = \int \frac{2hc^2}{\lambda^5} \frac{1}{e^{\frac{hc}{\lambda k T_{bb}}} + 1} d\lambda \quad (5)$$

where  $h$  is the Planck constant,  $k$  is the Boltzmann constant,  $c$  is the speed of light and  $\lambda$  is the wavelength. Gain and offset for each pixel are calculated such that all the pixels deliver the same signal when exposed to blackbodies at  $T_1$  and  $T_2$ . As the pixels' behavior is not rigorously linear, the table calculated will not be absolutely correct at temperature between  $T_1$  and  $T_2$ . This explains the W shape seen on measurements of RFPN, which is the remaining spatial noise after correction.

RFPN has been measured on commercial IRNova T2SL MWIR FPA (320x256 FPAs with 30 $\mu$ m pixel pitch). Measurements have been done using the following routine:

- Cooling down the FPA in the morning.
- One measurement when the FPA reaches its operating temperature (80K).
- One measurement at the end of the day.
- The cooling machine is turned off, bringing the FPA back to room temperature.

This makes 2 measurements a day, except for the first day when more measurements were done. For each measurement, gain and offset corrections were applied on each pixel, using the G/O tables determined on day D0.

We consider the correction is still valid as long as RFPN is lower than the temporal noise (TN) measured at a given day.

In the case of the IRNova FPA, results in Fig 7 show RFPN/TN for each measurement. We can see that even after 3 weeks, the correction can be deemed as valid, which means that the stability over time is excellent. The number of flickering pixels is also very low (typically 10 pixels across the full FPA).

This result means that a calibration can be made and does not need to be refreshed for a long time, which ultimately increases the IRFPA uptime (as the IR device has to be disabled during calibration phases). In some cases, the IR device could even be designed without on-board calibration device, which greatly impacts the Size Weight and Power (SWaP) issue.

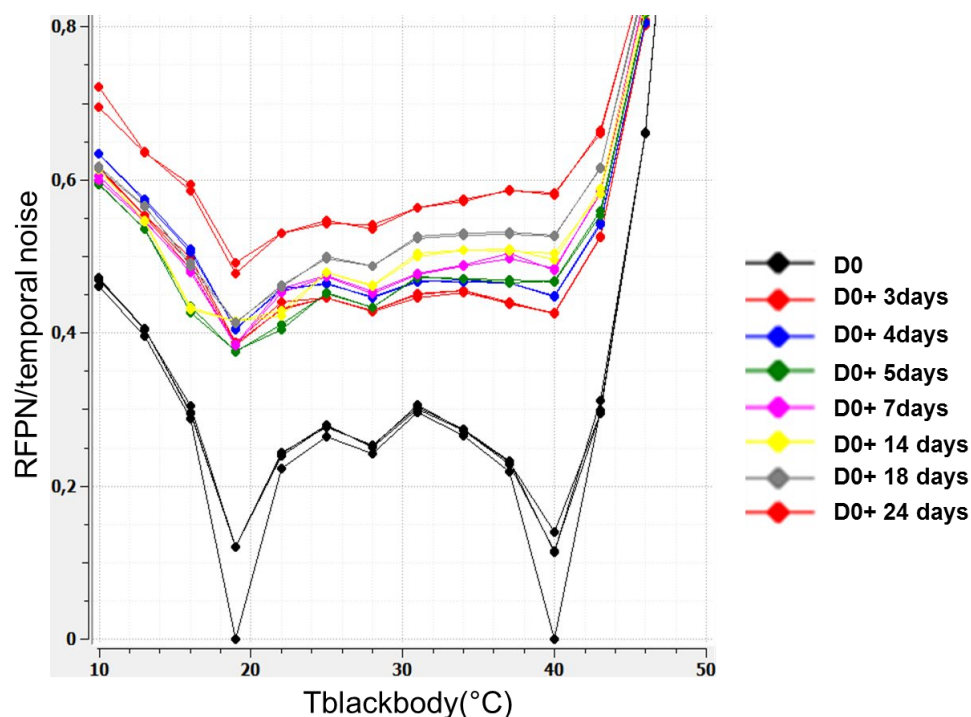


Fig 7 RFPN/rms using the same correction on different days

### B. Discussion

Results in terms of RFPN and number of flickering pixels seem very promising for T2SL technology, potentially ensuring long-term stability of infrared instruments absolute calibration.

In a more general manner, one may wonder whether RFPN is the most relevant figure of merit to faithfully depict stability over time. Indeed, RFPN highlights the nonlinearity of pixels. It may not be a major concern as long as the behavior is stable, thus correctable. This preliminary work shows that only using RFPN standards will not be enough to state on the “correctability” (or ability to be calibrated on the long-term) of the FPA. For example, flickering pixels (which may bias the “standard” pixel response used for corrections), may be overlooked as the RFPN cannot discriminate them (and apply proper correction to them). We may reach a scenario where RFPN is very low (if no flickering occurred during the calibration) and the resulting image however cannot be considered as stable. Complementary measurements are ongoing at ONERA, with the objective to define a measurement protocol to quantify the “correctability” of FPAs and to compare the merits of different competing technologies.

## V. POTENTIAL OF THE T2SL EMERGING TECHNOLOGY TO ADDRESS THE MWIR SPECTRAL DOMAIN

T2SL technology has initially drawn attention in the MWIR domain since it could potentially combine the advantages of MCT (high operating temperature) and InSb (excellent uniformity/stability) technologies, and thus potentially fulfill the SWaP (size, weight and power) requirements.

The electro-optic characterizations realized so far by different laboratories [2][10][11] [12][13][14] allow us to conclude that MWIR photodiodes and FPA exhibit a dark current higher than initially expected, typically 1000 times higher than the MCT state-of-the-art given by the Rule07 [9], making High Operating Temperature (HOT) MWIR out of reach for the time being. This high dark current has been attributed to low minority carriers lifetime (in the 80-100 ns range for T2SL in the MWIR domain), which is also responsible for the 80nm holes diffusion length reported in this paper. However, we have shown that a proper design of the active zone mitigates the impact of this low lifetime on QE values. The quantum efficiency of photodiodes is in the range of 50%, which is a very satisfying value, even if not as high as the 80% QE published in MCT technology. T2SL also proved to have no excess noise and flat angular response as well [1]. We also pointed out that the long-term stability of T2SL technology is excellent, such that T2SL could get back into the race for high performance infrared detectors in the MWIR domain.

However, we believe that it is interesting for T2SL to focus on the LWIR (8-12 $\mu$ m) and VLWIR (>12 $\mu$ m) spectral ranges. Indeed, there is a need for a technology that would offer good E-O performances (especially QE) with an excellent stability, few flickering pixels, and available in large format FPA. We believe that T2SL can address this need, since very promising results have been already reported with a LWIR megapixel T2SL FPA ( $\lambda_c=11\mu\text{m}@77\text{K}$  with 80% QE) [15] and a LWIR/VLWIR bispectral 320x256 FPA ( $\lambda_c=11\mu\text{m}@77\text{K}$  with QE in the range of 40% in both bands) [16]. LWIR T2SL photodiodes are currently being processed at IES and should be available for E-O characterization at ONERA very soon.

## V. CONCLUSION

In conclusion, we studied different T2SL MWIR photodiodes (from InAs-rich to GaSb-rich SL structures) in terms of quantum efficiency. Measurements pointed out a carrier collection issue as higher bias voltage improves the quantum efficiency in InAs-rich structure. Matching the results in the InAs-rich with Hovel equations, we found that the collection zone is smaller than the active zone because of low carrier diffusion lengths. Solutions have been proposed: 1) changing the minority carrier from hole to electrons which have better diffusion length, or 2) switching to backside illumination in order to match the active zone with the collection zone.

Experiments on an IRNova MWIR commercial T2SL FPA show that the stability over time is excellent based on RFPN measurements. It potentially ensures long-term stability of infrared instruments absolute calibration. This demonstrates that T2SL technology is competitive for high performance MWIR photodetection.

Finally, "Correctability" has been introduced as an alternative to RFPN measurements, aiming to depict the stability of FPAs over extended periods of time.

## VI. ACKNOWLEDGEMENTS

The authors acknowledge the financial support of the French procurement agency (DGA) and the LabEx FOCUS.

## REFERENCES

- [1] E. Giard, R. Talaat, M. Delmas, J.-B. Rodriguez, P. Christol, and I. Ribet-Mohamed, "Radiometric and noise characteristics of InAs-rich T2SL MWIR pin photodiodes," *J. Europ. Opt. Soc. Rap. Public.*, 9, 14022, 2014.
- [2] E. Giard, I. Ribet-Mohamed, J. Jaeck, T. Viale, R. Haïdar, R. Taalat, M. Delmas, J.-B. Rodriguez, E. Steveler, N. Bardou, F. Boulard, and P. Christol, "Quantum efficiency investigations of type-II InAs/GaSb midwave infrared superlattice photodetectors" *J. Appl. Phys.*, 116, 043101, 2014.
- [3] H. Hovel Semiconductors and Semimetals, vol.11, chap. 2, pp17–20, 1975.
- [4] Z.-B. Tian, E. Plis, R. Hinkey and S. Krishna, "Influence of composition in InAs/GaSb type-II superlattices on their optical properties". *Electronics Letters*, 50(23):1733–1734, 2014.
- [5] R. Rehm, M. Walther, J. Schmitz, F. Rutz, J. Fleißner, R. Scheibner and J. Ziegler, "InAs/GaSb superlattices for advanced infrared focal plane arrays". *Infrared Physics & Technology*, 52(6):344–347, 2009.



- [6] C. Cervera, J. B. Rodriguez, J. P. Perez, H. Ait-Kaci, R. Chaghi, L. Konczewicz, S. Contreras and P. Christol, "Unambiguous determination of carrier concentration and mobility for InAs/GaSb superlattice photodiode optimization", *J. Appl. Phys.* 106, 033709, 2009.
- [7] D.Hoffman, B.-M. Nguyen, P.-Y. Delaunay, A.Hood, M.Razeghi and J.Pellegrino "Beryllium compensation doping of InAs/GaSb infrared superlattice photodiodes". *Applied Physics Letters*, 91(14):143507–143507, 2007.
- [8] A.Brunner, L.Rubaldo, V. Destefanis, F. Chabuel, A. Kerlain, D. Bauza and N. Baier, "Improvement of RTS Noise in HgCdTe MWIR Detectors", *Journal of Elec Material*,43: 3060, 2014.
- [9] W.E. Tennant, D.Lee, M.Zandian, E.Piquette, M.Carmody. *Journal of Electrical Material* 37: 1406. doi:10.1007/s11664-008-0426-3, 2008.
- [10] M. Walther, J. Schmitz, R. Rehm, S. Kopta, F. Fuchs, J. Fleißner, W. Cabanski, J. Ziegler, "Growth of InAs/GaSb short-period superlattices for high-resolution mid-wavelength infrared focal plane array detectors", *Journal of Crystal growth*, 278(1):156–161, 2005.
- [11] Y.Weï, A.Hood, H.Yau, Gin, M.Razeghi, M. Z. Tidrow, and V.Nathan, "Uncooled operation of type-II InAs /GaSb superlattice photodiodes in the midwavelength infrared range", *Applied Physics Letters*, 86(23):233106-233106, 2005.
- [12] E.Plis, J.B.Rodriguez, H.Kim, G.Bishop, Y.Sharma, L.Dawson, S.Krishna, S.Lee, C.Jones and V.Gopal, "Type II InAs /GaSb strain layer superlattice detectors with p-on-n polarity" *Applied Physics Letters*, 91(13):133512–133512, 2007.
- [13] E.Aifer,J. Tischler,J.Warner, I.Vurgaftman, W.Bewley, J.Meyer, J.Kim, L.Whitman, C.Canedy and E.Jackson, "W-structured type-ii superlattice long-wave infrared photodiodes with high quantum efficiency". *Applied Physics Letters*, 89(5):053519–053519., 2006.
- [14] L.Höglund, A.Soibel, D.Z.Ting, A.Khoshakhlagh, C. J.Hill and S. D.Gunapala, "Minority carrier lifetime and photoluminescence studies of antimony-based superlattices", *SPIE Optical Engineering+ Applications*, pp.851106–851106. International Society for Optics and Photonics, 2013.
- [15] P.Manurkar, S.Ramezani-Darvish, B.-M.Nguyen, M.Razeghi, and J.Hubbs, "High performance long wavelength infrared mega-pixel focal plane array based on type-II superlattices", *Applied Physics Letters* 97, 193505 ; doi: 10.1063/1.3514244 ,2010.
- [16] E.-K.Huang, A.Haddadi, G.Chen, B.-M.Nguyen, M.-A. Hoang, R.McClintock, M.Stegall and M.Razeghi "Type-II superlattice dual-band LWIR imager with M-barrier and Fabry–Perot resonance," *Opt. Lett.* 36, 2560-2562, 2011.